ADMM-Based Distributed DC Optimal Power Flow with Power Flow Control

Xinyang Rui

Department of Electrical and Computer Engineering University of Utah Salt Lake City, UT, USA xinyang.rui@utah.edu

Mostafa Sahraei-Ardakani

Department of Electrical and Computer Engineering University of Utah Salt Lake City, UT, USA mostafa.ardakani@utah.edu

Mingxi Liu

Department of Electrical and Computer Engineering University of Utah Salt Lake City, UT, USA mingxi.liu@utah.edu

Thomas R. Nudell Smart Wires Inc. Durham, NC, USA Tom.Nudell@smartwires.com

Abstract—This paper presents a new methodology of incorporating power flow controllers, specifically flexible AC transmission systems (FACTS), into distributed DC optimal power flow (DCOPF). The distributed DCOPF problems are then solved by the alternating direction method of multipliers (ADMM). Efficient modeling of the power flow control capabilities of prominent FACTS devices, such as the unified power flow controller (UPFC) and the static synchronous series compensator (SSSC), enables the seamless integration of FACTS into the ADMM-based distributed DCOPF, thus allowing FACTS operation to be cooptimized with generator dispatch under a distributed control paradigm for the power system. The proposed ADMM-based distributed DCOPF problem with FACTS devices are studied through simulations on a 6-bus system and a modified IEEE 118-bus system to verify its convergence to the optimal generator dispatch.

Index Terms-Distributed DCOPF, ADMM, power flow control, FACTS devices.

NOMENCLATURE

Indices

Index of generators g

Index of transmission lines

Index of buses

u, v, m Index of subsystems

Parameters

 a_q, b_q, c_q Quadratic cost function parameters of generator g

Susceptance of line k b_k

Demand at bus n

Capacity of line k

Total number of subsystems

 n_k^{FACTS} The number of modular FACTS devices per phase on

Maximum active power output of generator q

This research was supported by the National Science Foundation under grant number 1756006.

978-1-6654-9921-7/22/\$31.00 ©2022 IEEE

 $\begin{array}{c} p_g^{\min} \\ V_k^{\mathrm{inj}} \\ V^{\mathrm{mod}} \end{array}$ Minimum active power output of generator qMaximum FACTS voltage injection on line k

Maximum voltage injection of a modular FACTS

device

Reactance of line k x_k

Sets \hat{K}

Set of lines equipped with FACTS, $\hat{K} \subset K$

Set of lines that are connected "to" bus n $\iota^+(n)$ $\iota^-(n)$ Set of lines that are connected "from" bus n

Set of generators connected to bus nG(n)

GSet of generators

KSet of transmission lines

N Set of buses

Variables

 Δb_k FACTS susceptance adjustment on line k

FACTS reactance adjustment on line k Δx_k

Bus voltage angle at the "from" bus of line k $\theta_{k,\text{fr}}$

 $\theta_{k,\mathrm{to}}$ Bus voltage angle at the "to" bus of line k

Active power flow on line k f_k

Active power output of generator g

I. Introduction

HE complexities of power system operation is increasing because of renewable energy penetration, power flow control technologies, demand response (DR) resources, etc. Moreover, the power grid is shifting towards a more distributed structure where independent entities are physically interconnected through transmission lines [1]. These factors cause difficulties for centralized control and operation of the power system. A more scalable, robust, and efficient alternative is the distributed control strategy [2], [3]. Therefore, the realization of solving power system operation models in a distributed manner is essential. One of the most important power system operation models is the optimal power flow (OPF), which minimizes the operation cost while considering system constraints. Power system operation requires OPF problems to be solved frequently and efficiently. Previous studies have discussed the advantages of distributed OPF over the traditional centralized OPF. Distributed OPF has lower requirements on communication infrastructure as it limits the amount of information exchanged [4], which also helps improve cyber security in the smart grid. In addition, distributed OPF has shown performance superiority in solving complex problems over large-scale networks [5].

To better utilize the transmission flexibility provided by flexible AC transmission system (FACTS) devices under the distributed control scheme, it is critical to incorporate them into distributed OPF. The power flow control capabilities of FACTS devices are important for improving the operation efficiency and available transfer capability (ATC) of the power grid [6]. Series FACTS devices can provide power flow control capabilities through adjusting the impedance of transmission lines. Previous studies have proposed distributed DCOPF formulations with the incorporation of FACTS devices [3], [5]. However, only variable-impedance FACTS devices, for which a prominent example is the thyristor-controlled series compensator (TCSC), that directly provide continuous impedance adjustments, are studied. Therefore, there is a necessity to incorporate other types of FACTS devices into distributed OPF. Different types of series FACTS devices rely on different methods to alter the effective reactance of transmission lines [7]. Prominent FACTS devices such as the unified power flow controller (UPFC) and the static synchronous series compensator (SSSC), which are both widely studied and used power flow control technologies, use voltage injections to effectively emulate reactance adjustments. UPFC is versatile [8] and is regarded as the latest generation of FACTS device [9]. Furthermore, SSSC devices are gaining rapid adoption through a light-weight and easy-to-deploy modular technology commercialized by Smart Wires Inc. [10]. In this paper, we focus on incorporating these types of FACTS devices into distributed OPF. For the remainder of this paper, we use the term "FACTS" is used to specifically refer to them.

Among the optimization methods for solving distributed OPF, the alternating direction method of multipliers (ADMM) has been utilized by many studies in recent years because of its suitability for solving large-scale, distributed optimization problems [4], [11], [12]. Several previous studies have focused on using ADMM to solve a variety of distributed OPF models. In [13], the authors developed a fully distributed and robust algorithm for ACOPF based on ADMM. In [4], a consensusbased ADMM approach for solving DCOPF with DR is presented. DCOPF is an approximate model of ACOPF and is widely used in market applications [14]. The effect of communication delay in ADMM-based distributed DCOPF is studied in [15]. In [16], a learning-aided asynchronous ADMM is proposed to better utilize computational resources when solving distributed OPF. The authors in [17] proposed a privacy preserving ADMM-based DCOPF algorithm and provided analysis for potential privacy leakage.

In this paper, we propose a distributed DCOPF formulation using the efficient FACTS modeling developed in [7] for the

incorporation of FACTS devices. The proposed distributed DCOPF with FACTS is solved using ADMM. To the best of the authors' knowledge, no existing literature focuses on solving distributed OPF with power flow control using ADMM.

The rest of this paper is organized as follows. Section II introduces the modeling of FACTS in DCOPF. The formulation and the algorithm of ADMM-based distributed DCOPF with FACTS is presented in Section III. In Section IV, the proposed model is studied through simulations on two different test systems. Finally, Section V concludes the paper.

II. MODELING OF FACTS DEVICES

In [7], linear modeling of various types of FACTS devices are presented for DC-based power system operation problems based on injection shift factors (ISF). The modeling of FACTS devices in this paper is adopted from [7], and is also equivalent to the DC model of SSSC presented in [18].

For a transmission line equipped with FACTS devices, the DC power flow equation is formulated as:

$$f_k = (b_k + \Delta b_k)(\theta_{k,\text{to}} - \theta_{k,\text{fr}}). \tag{1}$$

Alternatively, (1) can be formulated using reactance:

$$f_k = \frac{\theta_{k,\text{fr}} - \theta_{k,\text{to}}}{x_k + \Delta x_k}.$$
 (2)

As mentioned previously, series FACTS devices provide power flow control capabilities through altering the apparent impedance of transmission lines. Therefore, Δb_k and Δx_k are variables, resulting in nonlinearity in both (1) and (2). The constraints on Δb_k and Δx_k are dependent on device type. SSSC alters the line reactance by injecting a voltage that is in quadrature with the line current [19]. The magnitude of the voltage injection is controllable. Similarly, UPFC also provides series compensation through a voltage injection. The difference between UPFC and SSSC devices in altering the line reactance is that the angle of the UPFC voltage injection is also controllable. The series device of UPFC can be regarded as an SSSC [20], and it provides the maximum series compensation in magnitude when the voltage injection is in quadrature with the line current [7]. Therefore, in this paper, UPFC and SSSC share the same modeling for their operating ranges regarding line reactance adjustments.

In [7], the variation bounds of $\Delta b_k(\theta_{k,\text{to}} - \theta_{k,\text{fr}})$ for a line k equipped with FACTS devices is derived, which is presented as follows:

$$-V_k^{\text{inj}}|b_k| \le \Delta b_k(\theta_{k,\text{to}} - \theta_{k,\text{fr}}) \le V_k^{\text{inj}}|b_k|. \tag{3}$$

Eqns. (1) and (3) are nonlinear, which is highly undesirable in terms of computational efficiency. Moreover, their nonconvexity hinders the application in ADMM, as ADMM becomes a local optimization method when applied to solve nonconvex problems [12]. To address these issues, equivalently to the FACTS nodal injection model presented in [21], a variable ϕ_k is introduced to substitute $\Delta b_k(\theta_{k,\mathrm{to}}-\theta_{k,\mathrm{fr}})$. Eqns. (1) and (3) are then reformulated as:

$$f_k = b_k(\theta_{k,\text{to}} - \theta_{k,\text{fr}}) + \phi_k, \tag{4}$$

$$-V_k^{\text{inj}}|b_k| \le \phi_k \le V_k^{\text{inj}}|b_k|. \tag{5}$$

To validate the substitution, the equivalence between the DCOPF problems before and after the introduction of ϕ_k needs to be proved. Therefore, we first present the formulation of the DCOPF problem with FACTS using the nonlinear DC power flow equation (1), which is shown as follows:

$$P_{1}: \min \sum_{g \in G} (a_{g}p_{g}^{2} + b_{g}p_{g} + c_{g})$$
s.t.
$$(3);$$

$$p_{g}^{\min} \leq p_{g} \leq p_{g}^{\max}, \forall g \in G;$$

$$-f_{k}^{\max} \leq b_{k}(\theta_{k,\text{to}} - \theta_{k,\text{fr}}) \leq f_{k}^{\max}, \forall k \in K, k \notin \hat{K};$$

$$(8)$$

$$-f_{k}^{\max} \leq (b_{k} + \Delta b_{k})(\theta_{k,\text{to}} - \theta_{k,\text{fr}}) \leq f_{k}^{\max}, \forall k \in \hat{K};$$

$$(9)$$

$$\sum_{k \in \iota^{+}(n)} b_{k}(\theta_{k,\text{to}} - \theta_{k,\text{fr}}) - \sum_{k \in \iota^{-}(n)} b_{k}(\theta_{k,\text{to}} - \theta_{k,\text{fr}})$$

$$+ \sum_{k \in \iota^{+}(n), k \in \hat{K}} \Delta b_{k}(\theta_{k,\text{to}} - \theta_{k,\text{fr}}) - \sum_{k \in \iota^{-}(n), k \notin \hat{K}} \Delta b_{k}(\theta_{k,\text{to}} - \theta_{k,\text{fr}})$$

$$= d_{nt} - \sum_{g \in G(n)} p_{g}, \forall n \in N.$$

$$(10)$$

Eqn. (6) is the quadratic objective function which minimizes the total fuel cost. (3) is the aforementioned bounds of the impact of FACTS devices on power flow and is included in the formulation. (7) enforces the generator output constraints. (8) and (9) are transmission line thermal capacity limit constraints for lines without and with FACTS respectively. (10) specifies the power balance at each bus in the system.

Then, the DCOPF problem after the variable substitution is needed for comparison. The formulation is presented as follows:

$$P_{2}: \min \sum_{g \in G} (a_{g}p_{g}^{2} + b_{g}p_{g} + c_{g})$$
s.t.
$$(5), (8); - f_{k}^{\max} \leq b_{k}(\theta_{k,\text{to}} - \theta_{k,\text{fr}}) + \phi_{k} \leq f_{k}^{\max}, \forall k \in \hat{K};$$

$$\sum_{k \in \iota^{+}(n)} b_{k}(\theta_{k,\text{to}} - \theta_{k,\text{fr}}) - \sum_{k \in \iota^{-}(n)} b_{k}(\theta_{k,\text{to}} - \theta_{k,\text{fr}})$$

$$+ \sum_{k \in \iota^{+}(n), k \in \hat{K}} \phi_{k} - \sum_{k \in \iota^{-}(n), k \in \hat{K}} \phi_{k}$$

$$= d_{nt} - \sum_{g \in G(n)} p_{g}, \forall n \in N.$$

$$(11)$$

Eqn. (5) is the aforementioned constraint on ϕ_k to enforce the operating range of FACTS. (12) specifies the thermal

capacity limits on lines equipped with FACTS. (13) is the nodal balance constraints. Note that for modular FACTS (M-FACTS) devices, $V_k^{\rm inj}$ for line $k(k\in\hat{K})$ is related to the number of modules deployed on the line [7]:

$$V_k^{\text{inj}} = n_k^{\text{FACTS}} V^{\text{mod}}.$$
 (14)

Therefore, the proposed model can be utilized for M-FACTS operation under the distributed control scheme.

Contradiction is used to prove the equivalence between P_1 and P_2 . Suppose $\omega^* = \{\theta^*, p^*, \Delta b^*\}$ are the optimal solutions of P_1 . Then, for a line $k(k \in \hat{K})$, we can calculate ϕ_k^* as:

$$\phi_k^* = \Delta b_k^* (\theta_{k,\text{to}}^* - \theta_{k,\text{fr}}^*). \tag{15}$$

Using (15) and ω^* , we can form a feasible solution $\hat{\omega}^* = \{\theta^*, p^*, \phi^*\}$. Apparently, $\hat{\omega}^*$ is a feasible for P_2 . Let $\Gamma(\cdot)$ denote the objective function in (6). We now make the assumption that P_1 and P_2 are not equivalent, which means that there exists a solution $v = \{\theta, p, \phi\}$ for P_2 , where:

$$\Gamma(\mathbf{p}) < \Gamma(\mathbf{p}^*). \tag{16}$$

Again, for a line $k(k \in \hat{K})$, Δb_k can be calculated as:

$$\Delta b_k = \frac{\phi_k}{\theta_{k,\text{to}} - \theta_{k,\text{fr}}}.$$
 (17)

Combining (17) with v, a feasible solution for P_1 , $\hat{v} = \{\theta, p, \phi\}$ can be formed. As ω^* is the optimal solution for P_1 , we have:

$$\Gamma(p^*) \le \Gamma(p). \tag{18}$$

Eqn. (16) contradicts (18), implying that the assumption of P_1 and P_2 are unequivalent is false. Because of the convexity and linearity in constraints, we use P_2 to further derive the distributed DCOPF with FACTS, as well as applying ADMM for solving the model.

III. ADMM-BASED DISTRIBUTED DCOPF WITH FACTS

Following the approach in [4], DCOPF is reformulated to accommodate the application of ADMM. We use the decentralized ADMM with a central collector that handles the global variables [12]. Such approach is also utilized for distributed DCOPF in [22]. The power system is first divided into M subsystems. For each subsystem, there are local and coupling variables. Local variables are strictly only related to one subsystem. The other variables are all coupling variables. Each subsystem solves a subproblem independently and report the coupling variables to the central collector.

Coupling variables can be identified by examining the lines connecting different subsystems, which are referred to as boundary lines. Consider a boundary line k with node (k, fr) in subsystem v and (k, to) in subsystem v. Apparently, $\theta_{k, \text{fr}}$ and $\theta_{k, \text{to}}$ are both coupling variables. In addition, to locally solve the problems in v and u, these two variables need to be duplicated in the neighboring subsystem [4]. Thus, there are $\theta_{k, \text{fr}}$ and $\theta_{k, \text{to}}^v$ in v, as well as $\theta_{k, \text{to}}$ and $\theta_{k, \text{fr}}^u$ in u. The variables and their duplicates all are included in the full set of

coupling variables. A coupling variable and its duplicates are associated with the same global variable.

If FACTS devices are deployed on boundary line k, then ϕ_k is needed in both v and u to solve local problems in ADMMbased distributed DCOPF. Thus, ϕ_k^v and ϕ_k^u are coupling variables and are related to the same global variable. We can see that the previously presented FACTS modeling effectively facilitates the integration of FACTS in the ADMM-based distributed DCOPF. The general form consensus optimization [12] can be applied to formulate the ADMM-based distributed DCOPF. The formulation is presented as follows [4]:

$$P_3$$
:
$$\min \sum_{m=1}^{M} C_m(\boldsymbol{x}_m)$$
(19)

$$\boldsymbol{x}_m \in \xi_m, \forall m;$$
 (20)

$$\tilde{\boldsymbol{x}}_m - \tilde{\boldsymbol{z}}_m = 0, \forall m. \tag{21}$$

Eqn. (19) is the objective function which is the summation of the cost for all subsystems. In (20), ξ_m is the feasible region for variables in subsystem m. Therefore, (20) specifies the constraints for local and coupling variables in P2 for each subsystem. (21) specifies the relation between coupling variables and global variables. $ilde{z}_m$ is a linear function of the vector of global variables z [12].

The update rules of the ADMM are specified as [4], [12]:

$$\boldsymbol{x}_{m}^{j+1} = \underset{\boldsymbol{x}_{m} \in \xi_{m}}{\operatorname{argmin}} (\mathcal{C}_{m}(\boldsymbol{x}_{m}) + \boldsymbol{\lambda}_{m}^{jT} \tilde{\boldsymbol{x}}_{m} + \frac{\rho}{2} \|\tilde{\boldsymbol{x}}_{m}^{j} - \tilde{\boldsymbol{z}}_{m}^{j}\|_{2}^{2}), \forall m;$$
(22)

$$z_h^{j+1} = \frac{\sum_{\mathcal{G}(m,w)=h} (\tilde{\boldsymbol{x}}_m^{j+1})_w}{\sum_{\mathcal{G}(m,w)=h} 1}, \forall h;$$
 (23)

$$\boldsymbol{\lambda}_{m}^{j+1} = \boldsymbol{\lambda}_{m}^{j} + \rho(\tilde{\boldsymbol{x}}_{m}^{j+1} - \tilde{\boldsymbol{z}}_{m}^{j+1}), \forall m; \tag{24}$$

where λ_m^j is the vector of dual variables in iteration j. \mathcal{G} in (23) denotes the relationship that coupling variables correspond to a global variable. In (22), the problems are solved locally in each subsystem. The stopping criteria are [4]:

$$\|\boldsymbol{r}_{m}^{j+1}\|_{2}^{2} = \|\boldsymbol{\lambda}_{m}^{j+1} - \boldsymbol{\lambda}_{m}^{j}\|_{2}^{2} \le \epsilon_{1}, \forall m$$

$$\|\boldsymbol{s}^{j+1}\|_{2}^{2} = \rho \|\boldsymbol{z}^{j+1} - \boldsymbol{z}^{j}\|_{2}^{2} \le \epsilon_{2}.$$
(26)

$$\|\mathbf{s}^{j+1}\|_2^2 = \rho \|\mathbf{z}^{j+1} - \mathbf{z}^j\|_2^2 \le \epsilon_2.$$
 (26)

where ϵ_1 and ϵ_2 are the threshold values.

The algorithm is presented as follows [4]:

Algorithm 1 ADMM-based distributed OPF with FACTS

- 1: Initialize dual and global variables, set the threshold values for the stopping criterion;
- 2: Solve the optimization problem in (22) for each subsys-
- 3: Subsystems report coupling variable values, which include voltage phase angles and FACTS power injections, to the central collector;
- 4: The central collector updates global variables and sends them back to the subsystems;
- 5: If stopping criteria are satisfied at all subsystems, stop the algorithm. Otherwise, update the dual variables in each subsystem and go back to step 2.

IV. NUMERICAL STUDIES

The proposed model of ADMM-based distributed DCOPF with FACTS is tested in simulations on a 6-bus system as well as a modified IEEE 118-bus system. A two-way partition is applied to the 6-bus system and the 118-bus system is divided into 3 subsystems. Each iteration of ADMM is solved using IBM CPLEX 12.9 on a Intel Core i5 CPU with 8 GB of RAM.

For SSSC, we assume that each location of FACTS installation has a maximum voltage injection equivalent to two SmartValve 10-1800 modules installed, which is 11.32 kV [23]. Note that the M-FACTS devices are installed per phase, and the maximum voltage injection in real cases needs be multiplied by $\sqrt{3}$. The maximum voltage injection value is also used as the maximum voltage injection for UPFC devices.

A. 6-bus system results

The system data, presented in Table I-III, is taken from [4] with modifications.

TABLE I GENERATOR DATA OF THE 6-BUS SYSTEM

| Unit | nmin (MW) | p ^{max} (MW) | a | h | C |
|-------|------------|-----------------------|------|-------|-------|
| Ullit | p (IVI VV) | p (141 44) | a | U | C |
| 1 | 20 | 200 | 0.67 | 26.24 | 31.67 |
| 2 | 50 | 200 | 0.95 | 12.89 | 6.78 |

TABLE II Transmission line data of the 6-bus system

| Branch | From | To | x(p.u.) | f ^{max} (MW) |
|--------|------|----|---------|-----------------------|
| 1 | 1 | 2 | 0.6 | 150 |
| 2 | 1 | 3 | 0.6 | 50 |
| 3 | 2 | 4 | 0.1 | 150 |
| 4 | 3 | 5 | 0.1 | 150 |
| 5 | 4 | 5 | 0.1 | 150 |
| 6 | 1 | 6 | 0.1 | 150 |

TABLE III Load data of the 6-bus system

| Demand | Location (bus) | Load (MW) |
|--------|----------------|-----------|
| 1 | 3 | 150 |
| 2 | 4 | 150 |
| 3 | 6 | 10 |

Note that we changed the thermal limit of line 2 from 150 MW to 50 MW to increase the congestion in the system. The partition of the 6-bus system is shown in Table IV [4].

TABLE IV PARTITION OF THE 6-BUS SYSTEM

| Subsystem | Buses |
|-----------|-------|
| 1 | 1,6 |
| 2 | 2-5 |

FACTS devices are deployed on line 2 as it is a boundary line. The effectiveness of power flow control allows the cheaper generator 1 to produce more compared with the results obtained from DCOPF without FACTS. To verify that the ADMM-based distributed DCOPF converges to the optimal solution, the dispatch results are compared with the ones obtained from the DCOPF problem with nonlinear FACTS operating range. The full formulation is presented as follows:

$$P_{4}: \min \sum_{g \in G} (a_{g} p_{g}^{2} + b_{g} p_{g} + c_{g})$$
(27)

$$-f_{k}^{\max} \leq \frac{\theta_{k,\text{fr}} - \theta_{k,\text{to}}}{x_{k}} \leq f_{k}^{\max}, \forall k \notin \hat{K}, k \in K;$$

$$-f_{k}^{\max} \leq \frac{\theta_{k,\text{fr}} - \theta_{k,\text{to}}}{x_{k} + \Delta x_{k}} \leq f_{k}^{\max}, \forall k \in \hat{K};$$

$$(28)$$

$$-f_k^{\max} \le \frac{\theta_{k,\text{fr}} - \theta_{k,\text{to}}}{r_k + \Delta r_k} \le f_k^{\max}, \forall k \in \hat{K}; \tag{29}$$

$$-V_k^{\text{inj}} \le \frac{\Delta x_k(\theta_{k,\text{fr}} - \theta_{k,\text{to}})}{x_k} \le V_k^{\text{inj}}, \forall k \in \hat{K};$$
(30)

$$-V_k^{\text{inj}} \le \frac{\Delta x_k (\theta_{k,\text{fr}} - \theta_{k,\text{to}})}{x_k} \le V_k^{\text{inj}}, \forall k \in \hat{K};$$

$$\sum_{k \in \iota^+(n), k \notin \hat{K}} \frac{\theta_{k,\text{fr}} - \theta_{k,\text{to}}}{x_k} - \sum_{k \in \iota^-(n), k \notin \hat{K}} \frac{\theta_{k,\text{fr}} - \theta_{k,\text{to}}}{x_k}$$

$$+\sum_{k\in\iota^{+}(n),k\notin\hat{K}} \frac{\theta_{k,\text{fr}} - \theta_{k,\text{to}}}{x_{k} + \Delta x_{k}}$$

$$-\sum_{k\in\iota^{-}(n),k\in\hat{K}} \frac{\theta_{k,\text{fr}} - \theta_{k,\text{to}}}{x_{k} + \Delta x_{k}}$$

$$(31)$$

$$=d_n-\sum_{g\in G(n)}p_g, \forall n\in N.$$

Eqn. (30) is the operating range regarding the effective reactance adjustment [7]. Because of its nonconvexity and nonlinearity in constraints, P4 is solved using the IPOPT

Suppose that p_4^* is the optimal dispatch obtained by solving P_4 , and p_3^k is the dispatch reported by ADMM at iteration k, we can calculate the 2-norm estimated error (NEE) to show the convergence of ADMM to the optimal global generator dispatch as the iteration progresses. At iteration k, the NEE is calculated as:

$$NEE(k) = \sqrt{\frac{\sum_{g} ((\mathbf{p}_{4}^{*})_{g} - (\mathbf{p}_{3}^{k})_{g})^{2}}{|G|}}$$
(32)

where |G| is the total number of generators in the system.

For the 6-bus system, ρ is set to be 600. Threshold values ϵ_1 and ϵ_2 are both set to be 0.001. ADMM converged after 27 iterations. Fig. 1 shows how the value of NEE changes as the algorithm progresses, which verifies the convergence of the proposed ADMM-based DCOPF to the same result as P₄.

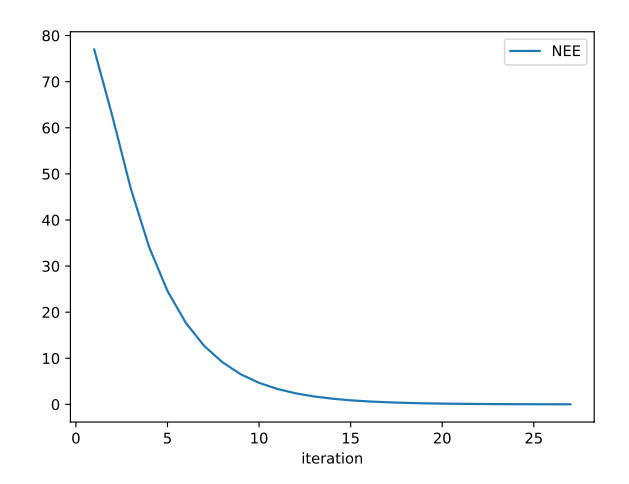


Fig. 1. NEE value of each iteration of ADMM-based DCOPF for the 6-bus

B. 118-bus system

The IEEE 118-bus test system data is available at [24], and modifications are made according to [25]. The partition of the system is presented in Table V [4].

TABLE V PARTITION OF THE 118-BUS SYSTEM

| Subsystem | Buses |
|-----------|--------------------|
| 1 | 1-32, 113-115, 117 |
| 2 | 33-73, 116 |
| 3 | 74-112, 118 |

FACTS devices are deployed on boundary lines 39 and 112. The value of ρ is set to be 1750. Threshold values ϵ_1 and ϵ_2 are both set as 0.001. The algorithm converged after 301 iterations. The progression of NEE is presented in Fig. 2. From the NEE results we can see that, for the 118-bus system, the NEE approaches 0 as the algorithm progresses, which verifies the convergence of the proposed model to optimal generator dispatch.

C. Discussion

The first interesting observation is that using per unit (p.u.) values facilitates the convergence of ADMM. Most implementations of DC power flow are based on the per unit system. However, in practice, if the base of power is multiplied at each side of the constraints, we can directly solve for the real values through DCOPF. For simulation studies in this paper, such an approach leads to slow convergence of ADMM compared to

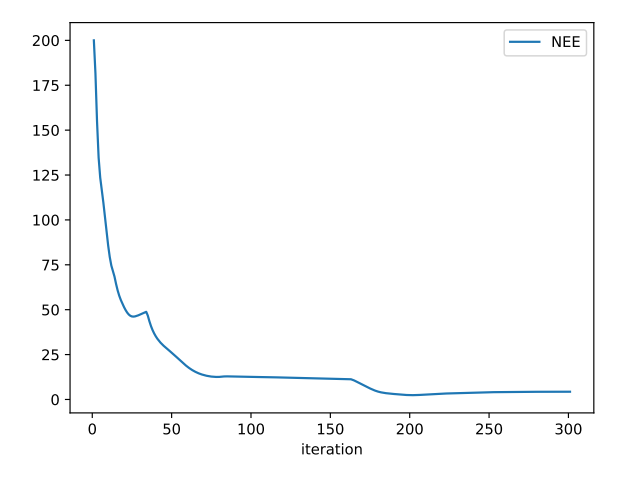


Fig. 2. NEE value of each iteration of ADMM-based DCOPF for the 118-bus system.

using p.u. values. If real values are used, ADMM takes more than 300 iterations to converge for the 6-bus system. For the 118-bus system, it could take more than 1500 iterations if ρ is not set very desirably. In addition, to achieve convergence within a reasonable number of iterations, ADMM requires a very large ρ value, e.g., $\rho > 50000$, for the 118-bus system.

Another observation is that the favorable ρ value of 20 in proposed by the authors of [4] is actually too small in our simulations and results in slow convergence.

V. CONCLUSIONS

In this paper, prominent series FACTS devices are integrated into the ADMM-based distributed DCOPF model. The developed model preserves the desirable feature of linearity and convexity of the original DCOPF problem, facilitating efficient co-optimization of FACTS point and generator dispatch under the distributed control scheme. The integration approach and the proposed model are validated by simulation studies conducted using different test systems. Simulation results shows the convergence of the ADMM algorithm when solving the proposed distributed DCOPF model.

Future research will include incorporating other types of series FACTS devices into the ADMM-based distributed DCOPF and modifying the ADMM algorithm to accommodate the computational challenges introduced by the modeling of certain types of FACTS devices.

REFERENCES

- A. Kargarian, J. Mohammadi, J. Guo, S. Chakrabarti, M. Barati, G. Hug, S. Kar, and R. Baldick, "Toward distributed/decentralized DC optimal power flow implementation in future electric power systems," *IEEE Transactions on Smart Grid*, vol. 9, no. 4, pp. 2574–2594, 2016.
- [2] J. Mohammadi, G. Hug, and S. Kar, "Role of communication on the convergence rate of fully distributed DC optimal power flow," in 2014 IEEE International Conference on Smart Grid Communications (SmartGridComm). IEEE, 2014, pp. 43–48.
- [3] ——, "Fully distributed DC-OPF approach for power flow control," in 2015 IEEE Power & Energy Society General Meeting. IEEE, 2015, pp. 1–5.

- [4] Y. Wang, L. Wu, and S. Wang, "A fully-decentralized consensusbased ADMM approach for DC-OPF with demand response," *IEEE Transactions on Smart Grid*, vol. 8, no. 6, pp. 2637–2647, 2016.
- [5] Q. Zhang and M. Sahraei-Ardakani, "Distributed dcopf with flexible transmission," *Electric Power Systems Research*, vol. 154, pp. 37–47, 2018
- [6] Y. Xiao, Y. Song, C.-C. Liu, and Y. Sun, "Available transfer capability enhancement using FACTS devices," *IEEE transactions on power systems*, vol. 18, no. 1, pp. 305–312, 2003.
- [7] X. Rui, M. Sahraei-Ardakani, and T. R. Nudell, "Linear modelling of series FACTS devices in power system operation models," *IET Generation, Transmission & Distribution*, vol. 16, no. 6, pp. 1047–1063, 2022.
- [8] J. Guo, M. L. Crow, and J. Sarangapani, "An improved upfc control for oscillation damping," *IEEE transactions on power systems*, vol. 24, no. 1, pp. 288–296, 2009.
- [9] H. Cai, L. Yang, H. Wang, P. Song, and Z. Xu, "Application of unified power flow controller (UPFC) in Jiangsu power system," in 2017 IEEE Power & Energy Society General Meeting. IEEE, 2017, pp. 1–5.
- Power & Energy Society General Meeting. IEEE, 2017, pp. 1–5.
 [10] Smart Wires Inc., "SmartValveTM," 2022, accessed: 2022-07-10.
 [Online]. Available: https://www.smartwires.com/smartvalve/
- [11] L. Yang, J. Luo, Y. Xu, Z. Zhang, and Z. Dong, "A distributed dual consensus ADMM based on partition for DC-DOPF with carbon emission trading," *IEEE Transactions on Industrial Informatics*, vol. 16, no. 3, pp. 1858–1872, 2019.
- [12] S. Boyd, N. Parikh, E. Chu, B. Peleato, J. Eckstein et al., "Distributed optimization and statistical learning via the alternating direction method of multipliers," Foundations and Trends® in Machine learning, vol. 3, no. 1, pp. 1–122, 2011.
- [13] T. Erseghe, "Distributed optimal power flow using ADMM," *IEEE transactions on power systems*, vol. 29, no. 5, pp. 2370–2380, 2014.
- [14] B. Stott, J. Jardim, and O. Alsaç, "Dc power flow revisited," *IEEE Transactions on Power Systems*, vol. 24, no. 3, pp. 1290–1300, 2009.
- [15] J. Xu, H. Sun, and C. J. Dent, "ADMM-based distributed opf problem meets stochastic communication delay," *IEEE Transactions on Smart Grid*, vol. 10, no. 5, pp. 5046–5056, 2018.
- [16] A. Mohammadi and A. Kargarian, "Learning-aided asynchronous admm for optimal power flow," *IEEE Transactions on Power Systems*, vol. 37, no. 3, pp. 1671–1681, 2021.
- [17] E. Liu and P. Cheng, "Mitigating cyber privacy leakage for distributed DC optimal power flow in smart grid with radial topology," *IEEE Access*, vol. 6, pp. 79181–7920, 2018.
- [18] S. Galvani, B. Mohammadi-Ivatloo, M. Nazari-Heris, and S. Rezaeian-Marjani, "Optimal allocation of static synchronous series compensator (SSSC) in wind-integrated power system considering predictability," *Electric Power Systems Research*, vol. 191, p. 106871, 2021.
- [19] X.-P. Zhang, C. Rehtanz, and B. Pal, Flexible AC transmission systems: modelling and control. Springer Science & Business Media, 2012.
- [20] D. Sen and P. Acharjee, "Optimal line flows based on voltage profile, power loss, cost and conductor temperature using coordinated controlled upfc," *IET Generation, Transmission & Distribution*, vol. 13, no. 7, pp. 1132–1144, 2019.
- [21] M. Sahraei-Ardakani and K. W. Hedman, "Computationally efficient adjustment of FACTS set points in DC optimal power flow with shift factor structure," *IEEE Transactions on Power Systems*, vol. 32, no. 3, pp. 1733–1740, 2016.
- [22] M. Ma, L. Fan, and Z. Miao, "Consensus ADMM and proximal ADMM for economic dispatch and AC OPF with SOCP relaxation," in 2016 North American power symposium (NAPS). IEEE, 2016, pp. 1–6.
- [23] Smart Wires Inc., "SmartValveTM 10-1800 v1.04," 2021, accessed: 2022-07-15. [Online]. Available: https://www.smartwires.com/download/20801/
- [24] Department of Electrical Engneering, Unviersity of Washington. Power systems test case archive. [Online]. Available: https://labs.ece.uw.edu/ pstca/pf118/pg_tca118bus.htm
- [25] S. Blumsack, Network topologies and transmission investment under electric-industry restructuring. Carnegie Mellon University, 2006.